

Active Control Based Energy Harvesting for Battery-Less Wireless Traffic Sensors: Theory and Experiments

K. Vijayaraghavan¹ and R. Rajamani^{1,*}

Abstract— This paper presents a novel battery-less wireless sensor that can be embedded in the road and used to measure traffic flow rate, speed and vehicle weight. Compared to existing inductive loop based traffic sensors, the new sensor is expected to provide increased reliability, easy installation and low maintenance costs. The sensor uses power only for wireless transmission and has ZERO idle power loss. Hence the sensor is expected to be extremely energy efficient. Energy to power this sensor is harvested from the short duration vibrations that results when an automobile passes over the sensor. Since all of the earlier work in literature on vibration energy harvesting has focused on continuous sources of vibration, this paper focuses on short duration vibrations and on developing low power control algorithms that can be implemented on the sensor using an analog circuit. To this effect this paper develops and compares three control algorithms “Fixed threshold switching”, “Maximum Voltage switching” and “Switched Inductor” for maximizing this harvested energy. The “Switched inductor” algorithm is shown to be the most effective at maximizing harvested energy. Experimental results are presented in the final section of the paper and show that adequate energy can be harvested from the passing of each axle of a vehicle to enable successful wireless transmission of data.

I. REVIEW OF CURRENT TRAFFIC SENSORS

Transportation agencies all around the country monitor traffic flow rates on most major highways using inductive loop detectors (ILDs). The Minnesota Department of Transportation (MnDOT) for example, monitors the flow rates at over 6000 points in the Minneapolis/St. Paul metro area using such ILDs. An ILD consists of a big loop of metallic coil buried in the lane. This loop is connected to a station which powers the loop and processes the information obtained from the loop to determine if a vehicle passes over the sensor. The flow rate information from such sensors is used to control ramp meters, identify congestion points, detect incidents and for a number of other applications.

Inductive loop detectors owe their popularity to their extremely high accuracy ([26]). Thus despite various new technologies for detecting vehicles such as image processing based detectors ([6],[13],[15]) and sound based systems ([2], [3]), inductive loop detectors remain the most widely used technology.

This work was supported in part by a research grant from the ITS Institute.

¹ K. Vijayaraghavan and R. Rajamani are with the Department of Mechanical Engineering, University of Minnesota, Minneapolis, MN 55455, USA

* rajamani@me.umn.edu, tel : (612) 626-7961, fax : (612) 625-4344.

Despite their popularity, ILDs are far from perfect and there has been considerable work to improve detection using better models, better filtering technology and by using better identification techniques such as Fuzzy Logic and Artificial Neural Networks (ANNs) ([1], [11], [24]). Despite many improvements, the installation of the ILD involves cutting a large section of the roadway in each lane and therefore causes considerable traffic disruption. Owing to its operating principle, the ILD needs to be continuously powered resulting in considerable idle power loss.

II. NEW TRAFFIC SENSORS

A. Overview

The researchers in this paper have developed a novel battery-less wireless traffic sensor, which is extremely energy efficient. The sensor is completely autonomous and can be embedded in the lane without the need for control/data cables. When an automobile passes over the sensor, a RF pulse is transmitted wirelessly to the station. By using different frequencies, several sensors can transmit to the same station. The sensor requires no external power source as it is powered by harvesting all its energy from vibrations that result when a vehicle passes over it. The sensor thus has ZERO idle power loss. Further this sensor has smaller dimension and can be installed with much lower traffic disruptions. This is especially true because the sensor does not need a power source and power lines do not need to be run to the sensor. This new sensor like the ILD, does not use complex image processing or audio processing techniques and would hence provide the same level of high reliability. Owing to the battery-less and wireless nature of the sensor low maintenance can also be expected. Further it is likely that the sensor can measure the number of axles and weight of passing vehicle in addition to the flow rate.

B. Principle

The proposed sensor is based on the principle of vibration energy harvesting (VEH) to enable wireless transmission of signals. Sodana et. al (2004) ([23]) provides a good review of many of these VEH techniques. Some of the earlier work has also focused on developing control algorithms to optimize the amount of energy harvested, ([14], [20]). However, the VEH techniques in literature focus predominantly on harvesting energy from a continuous source of vibration. However, when a

vehicle passes over the traffic sensor, the resulting mechanical vibrations are of short duration. Hence, although the concept of VEH is not new, it has never before been used to power a traffic sensor. Further the optimal algorithms that have been proposed earlier cannot be implemented in a stand-alone sensor as they require an external control input (and possibly an external power source). Hence new algorithms have been developed and implemented in this paper.

C. Hardware

The proposed sensor consists of a beam structure with a main beam and two support beams at the ends as shown in Figure 1. A total of four Piezo elements (two piezos for each of the support beams) are bonded at the locations shown in the Figure 1 and connected electrically in parallel. Ansys simulations have revealed that the average of the strain over the area of all the piezos depends only on the total load acting on the main beam. This configuration was chosen since the average voltage developed by the piezo would be independent of the locations of the load and the sensor can accurately determine the weight of the passing vehicle. It should be noted further that the speed of the passing vehicle can be measured by measuring the time difference in the loading between two consecutive sensors placed a short longitudinal distance apart. The number of axles on the vehicle is directly available, since each axle provides a load on the sensor and enables one wireless transmission per axle.

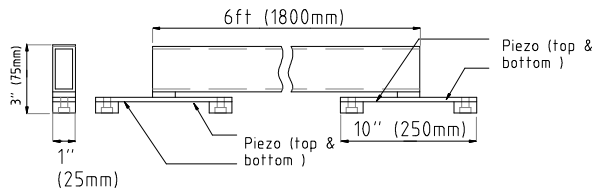


Figure 1: Sensor

D. Controller

In this paper, we develop a controller to optimize energy harvested from short duration vibration inputs from near impact loading. This technique could be extended to other applications such as shock absorbers and touch down of landing gear in airplanes. This paper further focuses on developing control strategies for the Energy Harvesting Systems (EHS), that is completely powered from the energy harvested and a controller that can be implemented onboard using simple analog electronics. The efficacy of these control strategies have been verified using simulations and experiments.

III. PROPOSED CONTROL SYSTEMS

A. Electrical Circuit

For the purpose of modeling, all the piezos are represented by a single piezo of equivalent parameters. This piezo electric energy harvesting element is modeled as a voltage source in series with a capacitor. The internal capacitance of the piezo is very small and the rate of

energy generated is also small. A typical energy harvesting circuit shown in Figure 2 consists of a storage capacitor to store the energy from the piezo. Over time the storage capacitor builds up voltage (equivalently sufficient energy) and is connected to the load (modeled as a resistor). The control strategy used for this switching determines the amount of energy harvested.

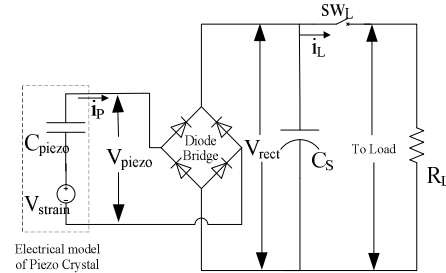


Figure 2: Energy harvesting circuit

B. System dynamics for energy harvesting

The voltage generated in the piezo causes a reaction force on the mechanical system. Hence the dynamics of the mechanical and electrical sub-systems are coupled. However the piezo element has dimensions of 75mm×75mm×0.191mm. Owing to the much smaller cross sectional area of the piezo element, the force exerted by the piezo is extremely small and the effect of the piezo force on the parent material can be neglected. Hence the mechanical dynamics can be decoupled from the electrical dynamics. For the purposes of this paper, in order to develop the control system, only the first mode of vibration is considered for the mechanical system. A more accurate model for the proposed structure can be developed from FEM analysis. The mechanical system, is modeled as a spring mass damper system by equation (1) and the strain is calculated from equation (2)

$$\ddot{u} + 2\zeta\omega_n\dot{u} + \omega_n^2 u = \frac{F}{m} \quad (1)$$

$$\varepsilon = \frac{u}{L} \quad (2)$$

where

u is the displacement of the mechanical system

L is the length scale associated with the mechanical system.

At low frequencies, the piezo electric material which is the critical part of the EHS, is modeled as a voltage source in series with a capacitance using equation (3) & (4) ([5],[18]). A more sophisticated model can be found in Weinbert et. al. ([29]). The overall dynamics of the system can be modeled by the dynamics of the mechanical system driving the electrical system.

$$V_{piezo} = V_{strain} - \frac{1}{C_{piezo}} \int i_p dt \quad (3)$$

$$V_{strain} = k\varepsilon \quad (4)$$

IV. SIMULATION RESULTS

For the simulations, it is assumed that the sensor beam

is modeled by a mechanical system having a mass of 100 kg, damping ratio of 0.7 and a spring constant of 10^6 N/m. These parameters were chosen so as to provide a natural frequency of 100 Hz in the simplified mechanical model. The load is assumed to be a square pulse of amplitude 3000N. The pulse is assumed to that starts at $t=2.9$ s and ends at $t=3$ s. The response of the mechanical system to this input is shown in Figure 3. The system was designed so that the Piezo would produce $V_{strain} = 60V$ for the static weight of the automobile. The switch shown in figure 2 is assumed to be an ideal switch that is turned on or off according to one of the control algorithms discussed below.

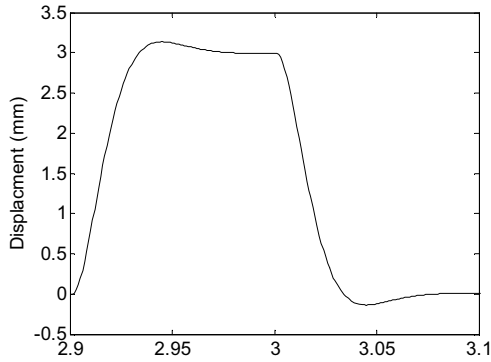


Figure 3: Mechanical response of the system

A. Fixed Threshold Switching

A typical EHS utilizes “Fixed Threshold Switching”, where in the switch SW_L is closed when the voltage of C_s exceeds a fixed threshold.

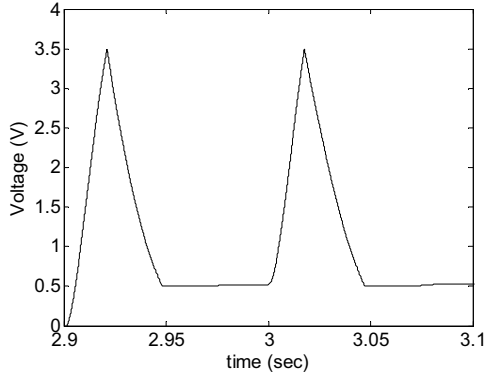


Figure 4: Voltage V_{C_s} for “Fixed Threshold switching” algorithm

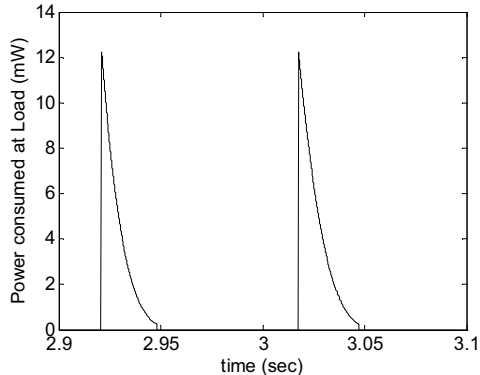


Figure 5: Instantaneous Power consumed by 1K Load with “Fixed Threshold switching algorithm”

The results from this strategy (Figures 4 and 5) are compared later to the new algorithms titled “Max Voltage Switching” and “Switched Inductor” which are shown to provide higher power to the load.

B. Max Voltage Switching

In this algorithm, the switch SW_L is closed when the voltage of C_s reaches a local maximum. The occurrence of maximum can be determined using analog electronics.

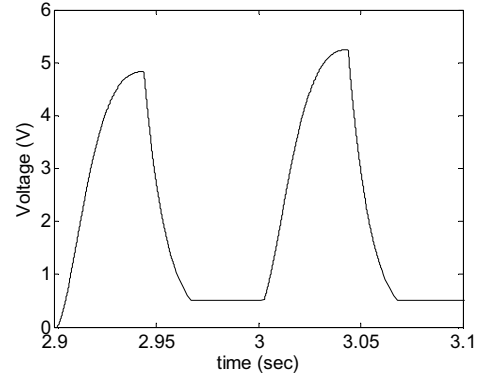


Figure 6: Voltage Output for “Max Voltage switching algorithm”

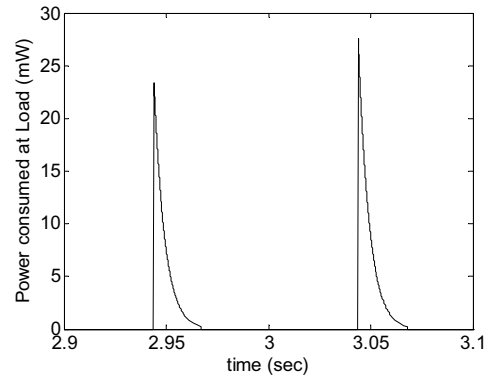


Figure 7: Instantaneous Power consumed by 1K Load with “Max Voltage switching algorithm”

This algorithm is more efficient at harvesting vibration energy than the simple fixed threshold algorithm described in the previous section. This is shown from the simulation results in Figures 6 and 7 and also from the calculations below. If displacement u is monotonic in $t \in [t_1, t_2]$, and the switch SW_L remains open in this time interval the charge transferred can be calculated by piece wise linear equations [29]. When the initial voltages are given by $V_{C_s}(t_1) = V_{C_s}^i$, $V_{C_{piezo}}(t_1) = V_{C_{piezo}}^i$, the voltages $V_{C_s}(t_2)$ and $V_{C_{piezo}}(t_2)$ at the end of the time interval can be calculated using equations (5-9) [29].

$$V_{strain}(t_{i+1}) = k \frac{u_{max}^{i+1}}{L} \quad (5)$$

$$V_{effective}(t_{i+1}) = \text{sign}(V_{strain}(t_{i+1}) - V_{C_{piezo}}(t_i)) \times \max \left(\begin{array}{l} |V_{strain}(t_{i+1}) - V_{C_{piezo}}(t_i)| \\ -V_{C_s}(t_i) - 2V_d \end{array} , 0 \right) \quad (6)$$

$$V_{C_{piezo}}(t_{i+1}) = \frac{C_s}{C_s + C_{piezo}} V_{effective}(t_{i+1}) + V_{C_{piezo}}(t_i) \quad (7)$$

$$V_{C_s}(t_{i+1}) = \frac{C_{piezo}}{C_s + C_{piezo}} |V_{effective}(t_{i+1})| + V_{C_s}(t_i) \quad (8)$$

$$V_{piezo}(t_{i+1}) = V_{strain}(t_{i+1}) - V_{C_{piezo}}(t_{i+1}) \quad (9)$$

C. Switched Inductor

This algorithm is an extension of the “Max Voltage Switching” algorithm presented in the previous section. This algorithm uses an inductor and additional switch SW_p . The presence of the inductor in the electrical circuit results in higher available voltage. If the time interval is partitioned into $[t_i, t_{i+1}]$ during which i_p does not change sign the charge transferred can be calculated by piece wise linear equations [29]. The amount of charge transferred is used to calculate the storage capacitor voltage at the end of each of those time steps giving rise to equations (10-13) [29].

$$V_{effective}^i = \text{sign}(V_s^{\max} - V_{C_{piezo}}^i) \times \max(|V_s - V_{C_{piezo}}^i| - V_{C_s}^i - 2V_d, 0) \quad (10)$$

$$Q_{\max}^i = C \times (1 + m) V_{effective}^i \quad (11)$$

$$V_{C_{piezo}}^{i+1} = V_{C_{piezo}}^i + Q_{\max}^i / C_{piezo} \quad (12)$$

$$V_{C_s}^{i+1} = V_{C_s}^i + |Q_{\max}^i| / C_s \quad (13)$$

where

$$m = \exp\left(-\pi\left(\zeta / \sqrt{1 - \zeta^2}\right)\right)$$

$$\zeta = R_d \sqrt{C/L}$$

$$C = C_p C_s / (C_p + C_s)$$

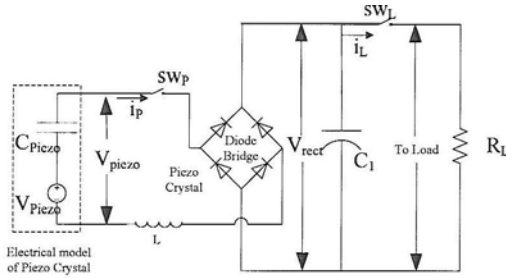


Figure 8: Energy harvesting with Inductor

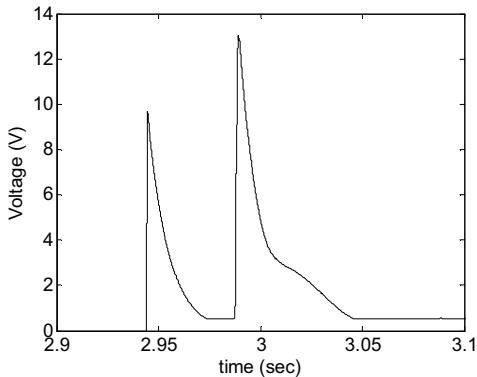


Figure 9: Voltage Output for “Switched Inductor” algorithm

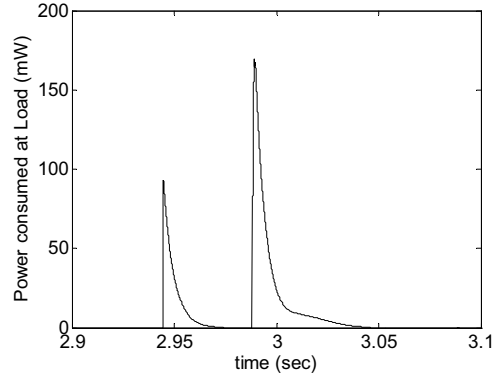


Figure 10: Instantaneous Power consumed by 1K Load with “Switched Inductor”

D. Effect of MOSFET on “Switched Inductor”

As mentioned in the earlier section, the max switch is implemented using simple analog electronics circuit. The circuit uses the voltage V_{C_s} stored in the storage capacitor to control a mosfet as shown in Figure 11. The points G, S and D respectively denote the gate, source and drain of the mosfet. In the “off” state, the mosfet offers nearly infinite resistance and accurately models an open switch. When the mosfet is turned “on” using a control signal, it offers a finite voltage drop V_{DS} which is a function of V_{C_s} . Since the control voltage is generated from the voltage stored in the storage capacitor, the effect of the mosfet in the “on” needs to be modeled. For simulations, the individual diodes in the bridge rectifier as well as the mosfet are modeled using the standard nonlinear equation ([8]).

$$V_{diode} = V_0 \ln\left(\frac{I_{diode}}{I_s} + 1\right) + I_{diode} R_{diode} \quad (14)$$

$$I_D = \begin{cases} 0 & \text{if } V_{GS} < V_T \\ 2k[(V_{GS} - V_T)V_{DS} - V_{DS}^2/2] & \text{if } V_{GS} > V_T \text{ and } V_{DS} < (V_{GS} - V_T) \\ k(V_{GS} - V_T)^2 & \text{if } V_{GS} > V_T \text{ and } V_{DS} > (V_{GS} - V_T) \end{cases} \quad (15)$$

where the subscripts

V_{GS} refers to the source-gate voltage

V_{DS} refers to the source-drain voltage

V_T is the mosfet threshold voltage

k is a mosfet constant

Clearly

$$V_{GS} = V_{DS} + V_{C_s} \quad (16)$$

Hence

$$V_{DS} = \begin{cases} -(V_{C_s} - V_T) + [(V_{C_s} - V_T)^2 + I_D/K]^{1/2} & \text{if } V_{C_s} > V_T \\ (I_D/K)^{1/2} - (V_{C_s} - V_T) & \text{otherwise} \end{cases} \quad (17)$$

The parameters for the model obtained from the corresponding data sheets are given below.

$$I_s = 2.7529 \times 10^{-15} A$$

$$V_0 = 0.0342 V$$

$$R_D = 1.1244 \Omega$$

$$V_T = 1.2 V$$

$$K = 9.685 \times 10^{-3}$$

$$L = 10 mH$$

$$R = 11.8 \Omega$$

R is the resistance of the inductor which is added in series. Figure 12 and Figure 13 compare the experimental response of the system to the theoretical model of the system for equivalent piezo parameters of $C_p = 1 \mu F$ and

$$V_{strain} = 50V$$

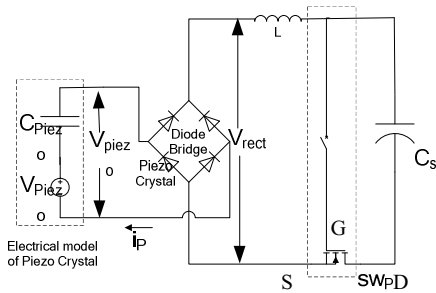


Figure 11: Mosfet in Max switch

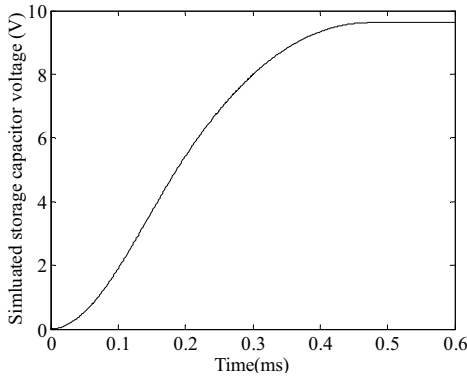


Figure 12: Simulation results

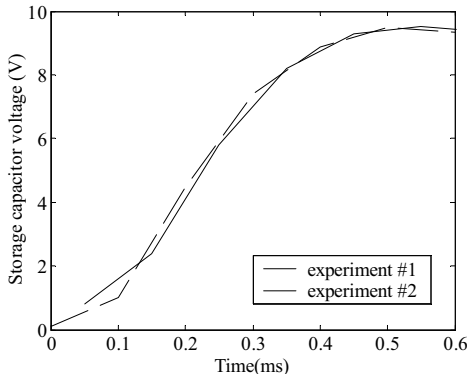


Figure 13: Results from two sets of experiment

Using this model, the theoretical voltage for the switched inductor is plotted versus the theoretical response of the max switch for the sensor in Figure 14 for

an initial storage capacitor voltage of 2.5V.

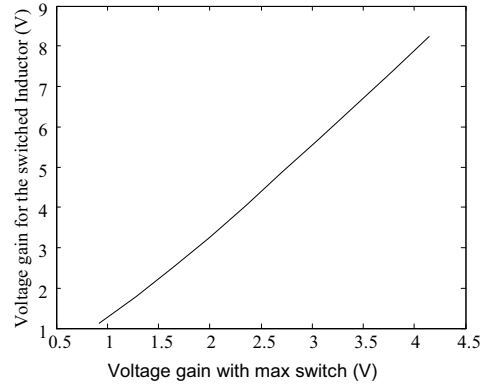


Figure 14: Theoretical voltage obtained from switched inductor vs the theoretical voltage obtained from max switching algorithm

V. EXPERIMENTAL RESULTS

Several experiments have been conducted in which the front and rear tires of a compact car were driven over the buried sensor. Owing to the unequal weight distribution in the car, the front and the rear tires apply different load on the sensor resulting in different voltages. Circuits implementing “Max Voltage Switching” and “Switched Inductor” were implemented. The load switch was disabled and the open circuit voltages generated at the storage capacitor were recorded. The data acquisition system has a range of $\pm 10V$. Hence the sensor was modified to generate a lower voltage at the storage capacitor. During the experiment, the max switch remains closed when V_{Cs} is lower than 3V. This feature has been used to illustrate that the “Switched Inductor” would offer negligible improvement if SW_p is improperly controlled. Figure 15 and Figure 16 shows the voltage generated using max switching algorithm. The voltage gain from the front tire is 2.5V and the voltage gain from rear tire is 1.75V. Figure 17 and Figure 18 show the voltage generated using the switched inductor algorithm. It is apparent that if SW_p is controlled as prescribed (for the rear tire), the “Switched Inductor” offers significant improvement. Further the voltage gain of roughly 3V, agrees with simulations.

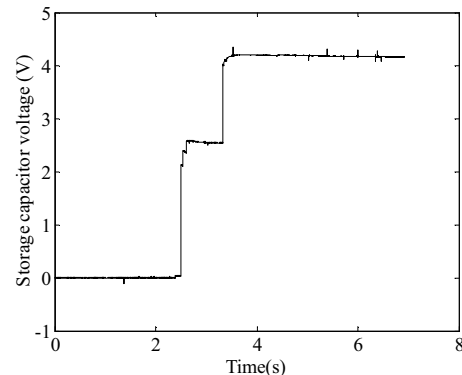


Figure 15: Max switching experiment 1

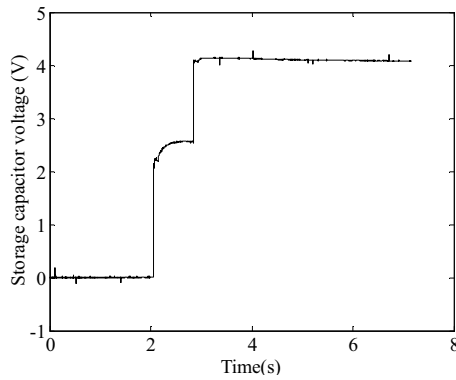


Figure 16: Max switching experiment 2

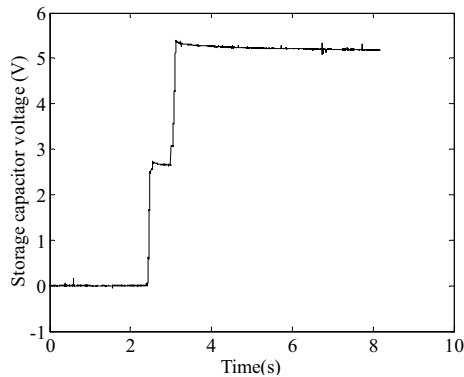


Figure 17: Switched inductor experiment 1

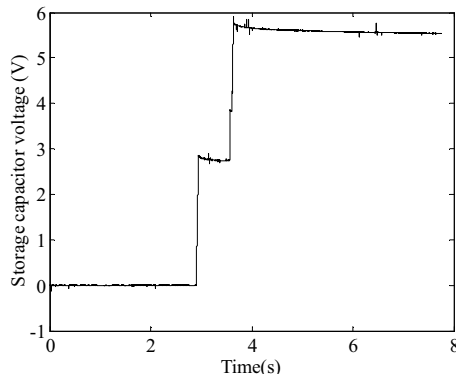


Figure 18: Switched inductor experiment 2

VI. REFERENCES

[1] C. Chen, J. Kwon, J. Rice, A. Skabardonis and P. Varaiya, "Detecting errors and imputing missing data for single-loop surveillance systems.", *Transp.Res.Rec.*, pp.160-167, 2003.

[2] S. Chen, Z. Sun and B. Bridge, "Traffic Monitoring Using Digital Sound Field Mapping", *IEEE Transactions on Vehicular Technology*, vol. 50, no. 6, pp.1582-1589, 2001.

[3] S. Chen, Z. P. Sun and B. Bridge, "Automatic traffic monitoring by intelligent sound detection", *Intelligent Transportation System, 1997.ITSC 97.IEEE Conference on*, pp.171-176, 1997.

[4] B. Coifman, "Improved Velocity Estimation Using Single Loop Detectors", *Transportation Research Part A: Policy and Practice*, vol. 35, no. 10, pp.863-880, 2001.

[5] C. W. De Silva, "Mechatronics: An Integrated Approach", CRC Press, 2004.

[6] N. Ferrier, S. Rowe and A. Blake, "Real-time traffic monitoring", *Applications of Computer Vision, 1994., Proceedings of the Second IEEE Workshop on*, pp.81-88, 1994.

[7] W. E. L. Grimson, C. Stauffer, R. Romano and L. Lee, "Using adaptive tracking to classify and monitor activities in a site",

Computer Vision and Pattern Recognition, 1998.Proceedings.1998 IEEE Computer Society Conference on, pp.22-29, 1998.

[8] P. Horowitz, W. Hill, "The art of electronics", Cambridge University Press, 1989.

[9] H. K. Khalil, "Nonlinear Systems", Upper Saddle River, New Jersey, Prentice Hall, 2002.

[10] S. W. Kim, Y. Eun, H. Kim, J. Ko, W. J. Jung, Y. Choi, Y. G. Cho and D. Cho, "Performance comparison of loop/piezo and ultrasonic sensor-based traffic detection systems for collecting individual vehicle information", *Proc.of 6th World Congress on ITS (CD-ROM)*, 1998.

[11] S. W. Kim, K. Kim, J. Lee and D. D. Cho, "Application Of Fuzzy Logic to Vehicle Classification Algorithm In Loop/Piezo-Sensor Fusion Systems", *Asian Journal of Control*, vol. 3, no. 1, pp.64-68, 2001.

[12] P. V. Kokotovic, J. O'Reilly and H. K. Khalil, "Singular Perturbation Methods in Control: Analysis and Design", Society for Industrial and Applied Mathematics Philadelphia, 1986.

[13] C. Li, K. Ikeuchi and M. Sakauchi, "Acquisition of Traffic Information Using Video Camera with 2D Spatio-Temporal Image Transformation Technique", *IEEE Intelligent Transportation*, pp.634-638, 1999.

[14] E. Lefeuvre, A. Badel, C. Richard, D. Guyomar, "Piezoelectric Energy Harvesting Device Optimization by Synchronous Electric Charge Extraction", *J Intell Mater Syst Struct*, vol. 16, no. 10, pp. 865-876, 2005.

[15] L.J. Mountain, J. B. Garner, "Application of photography to traffic surveys", *The Jour of the Inst. of Highway Engineers*, pp.12-19, 1980.

[16] P. T. Martin, Y. Feng and X. Wang, "Detector Technology Evaluation", *Mountain-Plains Consortium*, 2003.

[17] P. G. Michalopoulos and C. A. Anderson, "Costs and benefits of vision-based, wide-area detection in freeway applications", *Transp.Res.Rec.*, pp.40-47, 1995.

[18] O. D. Nwokah, "Mechanical Systems Design Handbook Modeling Measurement and Control", CRC Press, 2001.

[19] S. Oh, S. G. Ritchie and C. Oh, "Real Time Traffic Measurement from Single Loop Inductive Signatures", *81 stTRB Annual Meeting*, January, 2002.

[20] G. K. Ottman, H. F. Hofmann, A. C. Bhatt and G. A. Lesieutre, "Adaptive piezoelectric energy harvesting circuit for wireless remote power supply", *Power Electronics, IEEE Transactions on*, vol. 17, no. 5, pp.669-676, 2002.

[21] J. C. Rojas and J. D. Crisman, "Vehicle detection in color images", *Intelligent Transportation System, 1997.ITSC 97.IEEE Conference on*, pp.403-408, 1997.

[22] H. A. Sodano, D. J. Inman and G. Park, "Comparison of Piezoelectric Energy Harvesting Devices for Recharging Batteries", *J Intell Mater Syst Struct*, vol. 16, no. 10, pp.799-807, 2005.

[23] H. A. Sodano, D. J. Inman and G. Park, "A Review of Power Harvesting from Vibration Using Piezoelectric Materials", *The Shock and Vibration Digest*, vol. 36, no. 3, pp.197-205, 2004.

[24] C. Sun, S. G. Ritchie and S. Oh, "Inductive Classifying Artificial Network for Vehicle Type Categorization", *Computer-Aided Civil and Infrastructure Engineering*, vol. 18, no. 3, pp.161-172, 2003.

[25] Urban ITS Center at Polytechnic University Under sub-contract with Calspan University at Buffalo Research Center, "User's Manual For Cost Estimates of Intelligent Transportation Technologies (CEIT)",

[26] N. Ushio and T. Shimizu, "Loop vs ultrasonic in Chicago: Ultrasonic vehicle detector field test isolating diffused reflection and enduring harsh environment", *Proc.5th World Congr.Intelligent Transport Systems*, 1998.

[27] M. A. Vicencio, B. Qiu and M. G. Hartley, "Algorithms and architectures for the analysis of road-trafficmovements", *Image Processing and its Applications, 1989., Third International Conference on*, pp.182-186, 1989.

[28] K. Vijayaraghavan and R. Rajamani, "Active Control Based Energy Harvesting for Battery-Less Wireless Traffic Sensors," *Proceedings of the 2007 American Control Conference*.

[29] M.S. Weinberg, "Working equations for piezoelectric actuators and sensors", *Journal of Microelectromechanical Systems*, vol. 8, no4, pp. 529-533, 1999.